AIMS Energy, 3 (4): 774–797.
DOI: 10.3934/energy.2015.4.774
Received date 14 June 2015,
Accepted date 08 November 2015,
Published date 13 November 2015

http://www.aimspress.com/

Research Article

Thermodynamic analysis of methanation of palm empty fruit bunch (PEFB) pyrolysis oil with and without in situ CO_2 sorption

Hafizah Abdul Halim Yun * and Valerie Dupont

Energy Research Institute, School of Chemical and Process Engineering, The University of Leeds, LS2 9JT, UK

*** Correspondence:** Email: pmhahy@leeds.ac.uk; Tel: +44 (0) 113-343-2503;
Fax: +44 (0) 113-246-7310.

Abstract: Thermodynamic equilibrium analysis for conversion of palm empty fruit bunch (PEFB) bio-oil to methane using low-temperature steam reforming (LTSR) process was conducted by assuming either isothermal or adiabatic condition, with and without sorption enhancement (SE-LTSR), with $CaO_{(S)}$ or $Ca(OH)_{2(S)}$ as CO_2 sorbent. Temperatures of 300–800 K, molar steam to carbon (S/C) ratios of 0.3–7.0, pressures of 1–30 atm and molar calcium to carbon ratios (Ca:C) of 0.3–1.0 were simulated. For reasons of process simplicity, the best conditions for CH_4 production were observed for the adiabatic LTSR process without sorption at S/C between 2.5 and 3 (compared to the stoichiometric S/C of 0.375), inlet temperature above 450 K, resulting in reformer temperature of 582 K, where close to the theoretical maximum CH_4 yield of 38 wt % of the simulated dry PEFB oil was obtained, resulting in a reformate consisting of 44.5 vol % CH_4, 42.7 vol % CO_2 and 12.7 vol % H_2 and requiring only moderate heating mainly to partially preheat the reactants. Temperatures and S/C below these resulted in high risk of carbon by-product.

Keywords: palm empty fruit bunch bio-oil; low-temperature steam reforming; CO_2 sorption; methanation; thermodynamics; energy

1. Introduction

Bio-oil production via fast pyrolysis is one of the most attractive processes for converting solid biomass into renewable chemicals and higher value fuels [1,2] due to its feedstock flexibility. This process converts biomass into bio-oil (60–75 wt %), solid char (15–25 wt %) and gases

(10–20 wt %), depending on its feedstock and process parameters [3] by thermal decomposition of biomass in the absence of oxygen in the range of 350–550 ℃ [4,5] and reaction time of 0.5–5.0 s [3–5]. Bio-oils are easier to handle, store and transport [6] than the solid biomass they originate from. In addition, the calorific value of bio-oil exceeds that of the biomass source, i.e. an assessment has found that two truckloads of wood chips are equivalent to a single tanker load of bio-oil with the same energy content [7].

In 2004, bio-oil production was reviewed as a substitute for fuel oil or diesel for boilers, furnaces, engines and turbines in power plants [8]. However, CH_4 production is the main focus of the conversion of bio-oil for this study. The advantage of CH_4 is its high energy conversion efficiency and the already existing gas distribution infrastructure, as well as end-use technologies such as pipelines, power stations, heating and increasing numbers of cars running on compressed natural gas (CNG) in the world [9–12]. For example, the primary energy supply in Malaysia (Table 1) shows that natural gas consumes 53.6% of the total natural gas for power generators sector, as shown in Table 2. However, commercial and residential in the United Kingdom (UK) are the main consumer of natural gas, followed by power generators sector with 48% and 27%, respectively. Moreover, Malaysia exports approximately 19,537 Mtoe of liquefied natural gas (LNG), which makes Malaysia as the second largest exporter of LNG in the world after Qatar in 2014 [13]. Thus, for Malaysia, the conversion of bio-oil to CH_4 is a practical approach to meet the current energy demand in the country as CH_4 has a similar composition as natural gas.

Table 1. Primary energy supply in Malaysia in 2013 [14].

Energy source	Million tonne of oil equivalent (Mtoe)	Share percentage (%)
Natural gas	40.0	44.1
Oil	32.4	35.7
Coal	15.1	16.6
Hydro	2.7	3.0
Renewable	0.5	0.6
Total	90.7	100

Table 2. Share percentage (%) of natural gas consumption by sectors in 2013.

Sector	Malaysia [14]	United Kingdom [21]
Power generators	53.6	26.7
Non-energy	20.9	0.7
Industry	17.8	11.1
Self-generation	6.5	6.5
Commercial and residential	0.1	48.0
Other	1.1	7.0

The benefit of having CH_4 as the end product is in terms of a cleaner combustion process. A report compared the emissions of several harmful components which lead to environmental impacts by differentiating the type of fuels. It was found that CNG produced the lowest NO_x, CO and particulate matter (PM) compared to diesel, biodiesel, LNG and ethanol fuels [15]. CH_4 production from renewable sources is believed as a straightforward natural gas replacement since it has a similar composition to conventional natural gas [16]. In order to improve the penetration of renewables into

specific sectors of energy demand (e.g. power plants in Malaysia and domestic heating in the UK), as well as minimising the capital costs associated with changing the existing infrastructure for natural gas, it appears that converting bio-oil to methane may be more attractive than other alternative renewable liquid fuels like biodiesel. Thus, the potential of bio-oil as a renewable energy vector draws a number of researchers to investigate gaseous production from bio-oil as the feedstock [17–20].

Currently, CH_4 production from biomass can be split into two main methods, either biological or thermochemical (combustion, liquefaction, gasification and pyrolysis) processes. In Malaysia, biogas is commonly produced naturally from biological anaerobic degradation processes such as at municipal landfills and palm oil mill effluent (POME) anaerobic ponds. However, some disadvantages of landfill include limited land and the rising cost for municipal landfills [22], the lack of knowledge and also the absence of infrastructure availability in palm oil mill industries [23]. Thus, the potential of biogas production from the palm oil industry is not realised, and CH_4 escapes into the atmosphere, which contributes to global warming as CH_4 is 21 times more potent a greenhouse gas than CO_2 [24]. Moreover, some of the oil mill factories failed to meet the standardised discharge where unpleasant odours from anaerobic ponds offend local population [25]. Therefore, it seems that POME does not fulfil the requirement of Malaysia's National Green Technology Policy (2009) that emphasises promoting efficient utilisation of the technology, as well as conserving and minimising the impact on the environment [22]. For that reason, it is convenient to convert bio-oil to CH_4 via thermochemical means in dedicated plants where CH_4 fugitive emissions can be better controlled.

The gasification of wood illustrated in Figure 1 shows that syngas is produced from the beginning of the process in the gasifier, which then has to be reacted in the methanation process to produce biomethane [26]. The gasification stage, which operates at higher temperature (700–1000 ℃) [27], suffers from poor selectivity to gas products. The presence of CH_4 in the feed from the gasifier then adversely affects the equilibria towards methane consumption in the methanation process. An additional separation stage to the process would therefore be expected upstream of the methanation stage to prevent this. The general gasification for the conversion of biomass to methane thus appears energetically costly and complex. In addition, the multi-stage configuration would represent a safety challenge by providing multiple opportunities for potential leakage of CO (toxic) and H_2 (highly explosive) in addition to other flammable gases.

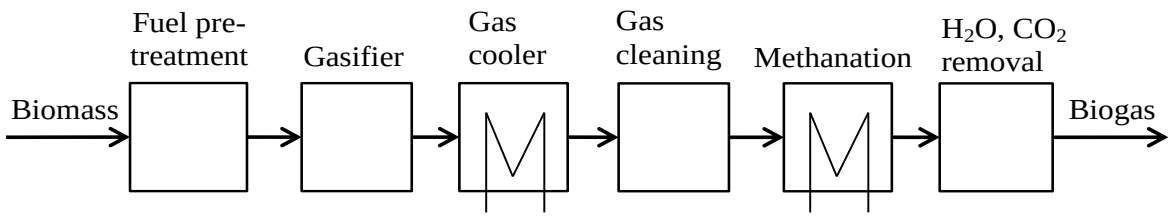

Figure 1. General gasification process for wood to biogas production.

In contrast, pyrolysis process requires lower temperature (within 350–550 ℃) [5,28] in order to convert biomass into bio-oil via fast pyrolysis. The products are easily separated according to their different phases; solids fall either to the bottom of the pyrolyser or collected by the cyclone at the top,

bio-oils are condensed by cooling, thus leaving the gases to evolve from the condenser separator. Solids can either be upgraded or re-used as fuels for pyrolysis's energy demand. Gases can join the methanate prior to the final separation stage, leaving the bio-oil as the sole feedstock for methanation in low-temperature steam reforming (LTSR). Bio-oils are volatiles and therefore would be well suited to catalytic methanation reaction technology, which is similar to industrial methanation of naphtha. Thus, it is convenient to utilise biomass in the form of pyrolysis oil for further reaction to produce CH_4.

The present work relies on chemical equilibrium calculations by using Chemical Equilibrium and Application (CEA) programme, where it is aimed to identify the optimum range of conditions for methane production from bio-oil feedstock in LTSR process. In addition, LTSR with in situ CO_2 sorption using $CaO_{(S)}$ or $Ca(OH)_{2(S)}$ is investigated for a PEFB bio-oil feedstock model in terms of CH_4 purity, yield and energy balances, and these processes are named 'sorption-enhanced LTSR' or SE-LTSR. Comparisons between LTSR and SE-LTSR are then performed with respect to their energy demand according to reforming temperature, molar steam to carbon ratio (S/C) and molar calcium to carbon ratio (Ca:C).

2. Materials and Methods

2.1. Description of palm empty fruit bunch (PEFB) bio-oil

In this research, bio-oil from the fast pyrolysis of palm empty fruit bunch (PEFB) was modelled as the feedstock for CH_4 production. PEFB bio-oil contains a great range of carboxylic acids, phenols, ketones, alcohols and aldehydes, in which acetic acid and phenol were found as the main compounds of PEFB bio-oil, in addition to many other oxygenated organics [18,29,30]. Since the exact composition of PEFB bio-oil is unknown, sensitivity analysis was first conducted to demonstrate that the results at chemical equilibrium for different PEFB bio-oil/H_2O systems are not sensitive to a precise bio-oil composition, provided the elemental content of PEFB bio-oil is well known. Table 3 shows the characteristics of PEFB bio-oil compositions with and without water content, where $C_{0.3238}H_{0.4957}O_{0.1798}N_{0.0007}$ of moisture free (mf) elemental formula was used as the basis for this study [30,31].

Table 3. Characteristics of PEFB bio-oil [30,31].

Water content, wt %	21.68	-
Elemental analysis, wt %		
Carbon	41.86	53.45
Hydrogen	7.82	6.88
Oxygen	50.22	39.54
Nitrogen	0.1	0.13
Molar formula	$C_{0.3821}H_{0.0060}O_{0.6108}N_{0.0011}$	$C_{0.3238}H_{0.4957}O_{0.1798}N_{0.0007}$

2.2. Methane production from bio-oil via steam reforming process

Several global reactions occur in producing CH_4 from bio-oil feedstock, where initially steam reforming reactions take place (R1–R2), followed by water-gas shift reaction (R3) and methane

synthesis (R4–R5). Reaction R6 collectively represents all the consecutive global reactions resulting in methane synthesis. By using matrices solution (Cramer's Rule), two main reactions for methane production from bio-oil which can be derived based on reactions (R3–R6) are expressed as reactions (R7) and (R8).

Steam reforming:

$C_nH_mO_k + (n - k)\ H_2O \rightarrow n\ CO + (n + 0.5m - k)\ H_2$ $\Delta H_{298\ K} > 0$ (R1)

$C_nH_mO_k + (2n - k)\ H_2O \rightarrow n\ CO_2 + (2n + 0.5m - k)\ H_2$ $\Delta H_{298\ K} > 0$ (R2)

Water-gas shift:

$CO + H_2O \leftrightarrows CO_2 + H_2$ $\Delta H_{298\ K} = -41.2$ kJ/mol CO (R3)

Methane synthesis:

$CO_2 + 4H_2 \leftrightarrows CH_4 + 2H_2O$ $\Delta H_{298\ K} = -165.0$ kJ/mol CH_4 (R4)

$2CO + 2H_2 \leftrightarrows CH_4 + CO_2$ $\Delta H_{298\ K} = -247.3$ kJ/mol CH_4 (R5)

$CO + 3H_2 \leftrightarrows CH_4 + H_2O$ $\Delta H_{298\ K} = -206.2$ kJ/mol CH_4 (R6)

Rearranging and combining (R1–R6), the global reactions of methane production from bio-oil become:

$C_nH_mO_k + (n - 0.25m - 0.5k)\ H_2O \rightarrow (0.5n - 0.125m + 0.25k)\ CO_2 + (0.5n + 0.125m - 0.25k)\ CH_4$ (R7)

$C_nH_mO_k + (2n/3 - m/6 - 2k/3)\ H_2O \rightarrow (2n/3 - m/6 + k/3)\ CO + (n/3 + m/6 - k/3)\ CH_4$ (R8)

Recently, a study has modelled a gasification process from biomass using calcium oxide (CaO) as a sorbent to capture carbon dioxide (CO_2) in gas production [32]. This work used biomass (straw) as a feedstock for CH_4 production, where the gasification system was simulated within 600–700 ℃ in the presence of CO_2 sorbent, at atmospheric pressure and followed by separate methanation stages (R4 & R6), in which temperature and pressure were kept constant at 300 ℃ and 10 bar, respectively. This is in contrast to our research, where bio-oil is used as a direct methanation feedstock due to its higher calorific value than biomass source. In addition, LTSR does not require multiple stages to produce CH_4. The novelty of our work is also in considering the presence of a CO_2 sorbent during the combined steam reforming/methanation reaction environment and not just steam gasification. Thus, the effects of in situ CO_2 capture can be gauged on the methane production mechanism rather than just the syngas production stage.

In the carbonation reaction (R9), CO_2 production from methanation synthesis (R5) reacts with CaO to produce calcium carbonate ($CaCO_3$), which results in higher purity of CH_4. Thus, CaO sorbent is expected to enhance the purity and also potentially the yield of CH_4 production from bio-oil via LTSR, which is investigated throughout this study. The following reactions are involved in the process featuring CO_2 sorption with $CaO_{(S)}$ and $Ca(OH)_{2(S)}$ sorbents:

Carbonation of $CaO_{(S)}$:

$CaO_{(S)} + CO_2 \leftrightarrows CaCO_{3(S)}$ $\Delta H_{298\ K} = -178.2$ kJ/mol CO_2 (R9)

Carbonation of $Ca(OH)_{2(S)}$:

$Ca(OH)_{2(S)} + CO_2 \leftrightarrows CaCO_{3(S)} + H_2O$ $\Delta H_{298\ K} = -69.0$ kJ/mol CO_2 (R10)

By combining the results of R7 and R9 in the global reaction of LTSR with the in situ CO_2 sorption via CaO sorbent (R11), as well as via the $Ca(OH)_{2(S)}$ sorbent (R12), both approaches can achieve a reformate consisting of pure CH_4:

$$C_nH_mO_k + (n - 0.25m - 0.5k)\ H_2O + (0.5n - 0.125m + 0.25k)\ CaO_{(S)} \rightarrow (0.5n - 0.125m + 0.25k)\ CaCO_{3(S)} + (0.5n+0.125m-0.25k)\ CH_4 \quad \text{(R11)}$$

$$C_nH_mO_k + (0.5n - 0.125m - 0.75k)\ H_2O + (0.5n - 0.125m + 0.25k)\ Ca(OH)_{(2S)} \rightarrow (0.5n - 0.125m + 0.25k)\ CaCO_{3(S)} + (0.5n + 0.125m - 0.25k)\ CH_4 \quad \text{(R12)}$$

2.3. Methodology of thermodynamic equilibrium calculations

The Chemical Equilibrium and Applications (CEA) code was used in this work to obtain the chemical equilibrium compositions for assigned thermodynamic states, such as temperature and pressure, or system enthalpy and pressure. CEA's solution method is based on the minimisation of Gibbs energy from a chosen set pool of reactants and equilibrium products of known thermodynamic properties, as opposed to an assumed set of reactions with known equilibrium constants. This offers an advantage to this work, provided that the chosen pool of products is comprehensive, no assumptions are made towards which reactions have taken place to reach equilibrium. At first, the simulations of this work are mainly focused towards the constant temperature and pressure conditions. Isothermal and isobaric conditions are close to those of a packed-bed reactor with negligible pressure drop across the reactive zone where, in the case of an exothermic process, cooling would be applied throughout the reactor to maintain a controlled, constant temperature. Additional simulations were performed later with constant enthalpy and pressure, simulating a well-insulated reactor whose temperature evolves from a set initial value to a higher one in the case of an exothermic process, or to a lower one for an endothermic process. The equations based on the minimisation of Gibbs energy presented in CEA [33] are nonlinear in the composition variables and thus, CEA relies on the iteration procedure that utilises Newton-Raphson method to solve the corrections to initial estimates of compositions and moles of gaseous species [34]. CEA allows the inclusion of condensed species (liquids and solids), therefore solid CO_2 sorbents like $CaO_{(S)}$, $Ca(OH)_{2(S)}$ and $CaCO_{3(S)}$ are able to be considered in the systems studied. In addition, a user can expand the thermodynamic data library with new compounds such as bio-oil model chemicals (e.g. phenol, levoglucosan, acetic acid, etc.).

The CEA programme presents results in terms of mole fractions in the equilibrium mixture. In order to easily determine the total molar output at equilibrium, argon (Ar) was used in the initial reactant mixture with 0.01 mole fraction so that an Ar balance would provide directly the total molar output at equilibrium, as expressed by equation (1). As the amount of Ar chosen is negligible, it is assumed that the equilibrium mixture is not affected by the presence of Ar.

Number of moles produced for species "i":

$$n_i = y_{i,out} \times n_{total,out} \quad (1)$$

where:

$y_{i,out}$ = mole fraction for species i produced, output of CEA;

$n_{total,out}$ = total number of moles produced, $n_{Ar,in}/y_{Ar,out.}$

The overall enthalpy balance (ΔH_{Tot}), i.e. the heat demand for methane production is the sum of the enthalpy change terms for each reactant (PEFB bio-oil ΔH and H_2O ΔH) and reaction enthalpies. The reactant enthalpy terms consist in bringing the feed species bio-oil and water from ambient temperature (298 K, 1 atm) in their natural phases to the chosen reformer temperature (T), and reaction enthalpies are the enthalpy change between equilibrium mixture and feed at T, as well as sorbent related reactions. We assume here that if the process operates with excess steam (by way of S/C or $Ca(OH)_{2(S)}$), the unreacted steam is then recycled to the reformer, and only the net amount of H_2O feed requires heating from ambient temperature, liquid phase to vapour phase at T. In addition, when simulating the sorption-enhanced LTSR with in situ CO_2 capture (SE-LTSR), it is assumed that the carbonate is subsequently calcined to $CaO_{(S)}$ at T. In the case of $CaO_{(S)}$ as the CO_2 sorbent, it is then returned straight to the reformer at T. When using $Ca(OH)_{2(S)}$ as the sorbent, the enthalpy change of rehydrating $CaO_{(S)}$ to $Ca(OH)_{2(S)}$ with the net amount of water is taken into account in the overall enthalpy balance. Rehydration of $CaO_{(S)}$ at T takes place first with excess water vapour also at T, and then, the remainder of $CaO_{(S)}$ at T is hydrated with net liquid water at ambient temperature. These assumptions reflect ideal conditions of heat integration by ignoring the thermal efficiencies of the recycling processes (water, sorbent) and the practicalities of calcination. The latter would require higher temperature (typically 1170 K for Ca-sorbents), followed by heat recuperation measures. Nevertheless, these ideal conditions allow closer comparisons between LTSR and SE-LTSR processes without going into more comprehensive process modelling where auxiliary units would have to be depicted together with their heat losses (fluid and solids movers, piping and valves, heat exchangers). The data of enthalpy in standard conditions (298 K and 1 atm) were obtained from the National Institute of Standards and Technology (NIST) and also from the thermodynamic properties database file 'thermo.inp' in the CEA programme.

Individual enthalpy change calculations were carried out using the enthalpy of individual species (i.e. CH_4, CO_2, CO, H_2, C(gr), H_2O, phenol and acetic acid). Equation (2) was used when using NIST data where equation (3) was used for the data taken from the CEA programme.

$$H^o = (At) + \left(\frac{Bt^2}{2}\right) + \left(\frac{Ct^3}{3}\right) + \left(\frac{Dt^4}{4}\right) + \left(\frac{E}{t}\right) + F - H \quad (2)$$

$$\frac{H^o}{RT} = \left(-a_1 T^{-2}\right) + \left(a_2 T^{-1} \ln T\right) + a_3 + \left(\frac{a_4 T}{2}\right) + \left(\frac{a_5 T^2}{3}\right) + \left(\frac{a_6 T^3}{4}\right) + \left(\frac{a_7 T^4}{5}\right) + \left(\frac{b_1}{T}\right) \quad (3)$$

where:
H^o = standard enthalpy of formation (kJ/mol);
t = reaction temperature (K)/1000;
T = reaction temperature (K);
R = gas constant (8.3144621×10^{-3} kJ/mol.K).

The calculations for reactant enthalpy changes of PEFB bio-oil ΔH, H_2O ΔH, and the enthalpy of reaction expressed by equations (4–7) were used to determine the energy required or released for the overall reactions in producing one mole of CH_4 from PEFB bio-oil feedstock. Enthalpy change of decarbonation of $CaCO_3$ back to CaO is represented by equation (8).
ΔH reactants (kJ/mol CH_4 produced):

$$\text{PEFB bio oil } \Delta H = {n_{oil,in} \times \left(H_{oil,T} - H_{oil,298K}\right)} \Big/ {n_{CH_4,out}} \quad (4)$$

$$H_2O\ \Delta H = {n_{H_2O,net} \times \left(H_{H_2O,T} - H_{H_2O,298K}\right)} \Big/ {n_{CH_4,out}} \quad (5)$$

where $n_{H_2O,net} = n_{H_2O,in} - n_{H_2O,out}$.

Summing up all reactant enthalpies:

$$\text{Reactants } \Delta H = \text{PEFB bio oil } \Delta H + H_2O\ \Delta H \quad (6)$$

ΔH of reaction (kJ/mol CH_4 produced):

$$\text{Reaction } \Delta H = \left(\sum H_{products,T} - \sum H_{reactants,T}\right) / n_{CH_4,out} \quad (7)$$

ΔH of decarbonation (kJ/mol CH_4 produced):

$$\text{Decarb } \Delta H = {n_{CaCO_3,out} \times \left(H_{CaO,T} + H_{CO_2,T} - H_{CaCO_3,T}\right)} \Big/ {n_{CH_4,out}} \quad (8)$$

When using $CaO_{(S)}$ as the sorbent, $Ca(OH)_{2(S)}$ formed in the reformer and not carbonated due to excess Ca compared to CO_2 product will require dehydration (calcination) before recycling:

$$\text{DeHy } \Delta H = n_{Ca(OH)_{2(S)},out} \times \left(H_{CaO_{(S)},T} + H_{H_2O,T} - H_{Ca(OH)_{2(S)},T}\right) \quad (9)$$

However, when using $Ca(OH)_{2(S)}$ as the sorbent, this term is zero as excess $Ca(OH)_{2(S)}$ is directly recycled to the reformer.

Rehydration with excess water, when $n_{H_2O,out} < n_{CaCO_{3(S)},out}$:

$$\text{ReHy1}\Delta H = n_{H_2O,out} \times \left(H_{CaO_{(S)},T} + H_{H_2O,T} - H_{CaCO_{3(S)},T}\right) \quad (10.1)$$

Rehydration with net water:

$$\text{ReHy2}\Delta H = \left(n_{CaCO_{3(S)},out} - n_{H_2O,out}\right) \times \left(H_{CaO_{(S)},T} + H_{H_2O(liq),298K} - H_{CaCO_{3(S)},T}\right) \quad (10.2)$$

where:

$n_{oil,in}$ = number of moles of PEFB bio-oil feed;

$n_{CH_4,out}$ = number of moles of CH_4 produced;

$n_{H_2O,in}$ = number of moles of water feed;

$n_{CaCO_3,out}$ = number of moles of $CaCO_3$ produced;

H = enthalpy in kJ/mol;
T = reformer temperature (K).

Finally, total enthalpy process:

$$\Delta H_{Tot} = \text{Reactants } \Delta H + \text{Reaction } \Delta H + \text{Decarb } \Delta H + \text{DeHy } \Delta H + \text{ReHy1} \Delta H + \text{Rehy2} \Delta H \quad (11)$$

3. Results and Discussion

3.1. Palm empty fruit bunch (PEFB) bio-oil composition and choice of model bio-oil

The bio-oil mixture is represented in $C_nH_mO_k$ elemental format since the bio-oil composition is too complex to determine the precise amount of different compounds in the bio-oil. A sensitivity analysis for bio-oil composition was conducted using $C_{0.3238}H_{0.4957}O_{0.1798}N_{0.0007}$ from reference [31] as the basis for elemental content of PEFB bio-oil approximated by different values of mole fractions of acetic acid, phenol and levoglucosan.

The CEA programme predicted CH_4 production using the same value of total feed of 3000 moles of carbon for all the conditions tested and in the temperature range of 300–800 K at 1 atm. Three different PEFB model bio-oil mixtures consisting of acetic acid, phenol and levoglucosan were used to simulate the target bio-oil elemental composition $C_{0.3238}H_{0.4957}O_{0.1798}N_{0.0007}$, which are listed in Table 4. These were then tested for a range of temperatures and S/C in equilibrium LTSR at atmospheric pressure to assess the sensitivity of CH_4 yield to the model mixture make up (Figure 2). Based on CH_4 production from bio-oil reaction (R7), the predicted equilibrium CH_4 yield was calculated using equation (12), whereas the percentage error was calculated via equation (13).

$$CH_4 \text{ yield} = 100 \times M_{CH_4} \times n_{CH_4,out} \Big/ \left(M_C \times n_{C,in}\right) + \left(M_H \times n_{H,in}\right) + \left(M_O \times n_{O,in}\right) \quad (12)$$

Percentage error for bio-oil of composition between the target and the model bio-oil is:

$$\text{Error (\%)} = 100 \times \left[1 - \text{max } CH_4 \text{ yield for model bio oil} \Big/ \text{max } CH_4 \text{ yield for target bio - oil}\right] \quad (13)$$

where:

M_{CH_4} = molar mass of CH_4;

M_C = molar mass of carbon element in bio-oil;
M_H = molar mass of hydrogen element in bio-oil;
M_O = molar mass of oxygen element in bio-oil;

and the maximum CH_4 yield is that obtained from complete reaction R7 using LTSR or complete reactions R11 or R12 using SE-LTSR for a given bio-oil.

Table 4 lists three very distinct mixtures of the model compounds (acetic acid, phenol and levoglucosan) that are known to feature significantly in PEFB bio-oil composition from experiments [18]. Each mixture (M1, M2 and M3) was modelled in order to achieve an elemental formula closest to that of the target material $C_{0.3238}H_{0.4957}O_{0.1798}N_{0.0007}$ as in Table 3. It can be seen

that despite significant differences in the amount of acetic acid, phenol and levoglucosan, each mixture results in a theoretical maximum CH_4 yield of less than 3% error with the target material. Figure 2 shows that the equilibrium CH_4 yields calculated using equation (12) for the temperature range (400–800 K) and the three model mixtures (M1–M3) defined in Table 2 were very similar for a given S/C and temperature. Note the intended mixture elemental formula had a theoretical maximum CH_4 yield of 39.5 wt % of $C_nH_mO_k$ feed. Thus, the LTSR process does not appear to be sensitive to an exact composition of bio-oil feedstock as long as its elemental content remains the same.

Table 4. Estimation for three different PEFB bio-oil compositions based on the intended elemental formula $C_{0.3238}H_{0.4957}O_{0.1798}N_{0.0007}$.

Mixture	M1	M2	M3
Mole fraction:			
Acetic acid	0.55	-	0.7
Phenol	0.3	0.41	0.3
Levoglucosan	0.15	0.59	-
Molar formula	$C_{0.3319}H_{0.4803}O_{0.1878}$	$C_{0.3386}H_{0.4718}O_{0.1896}$	$C_{0.3368}H_{0.4842}O_{0.1789}$
CH_4 yield wt % (Eq.12)	38.44	38.31	39.97
Error % (Eq.13)	2.7	3	1.1

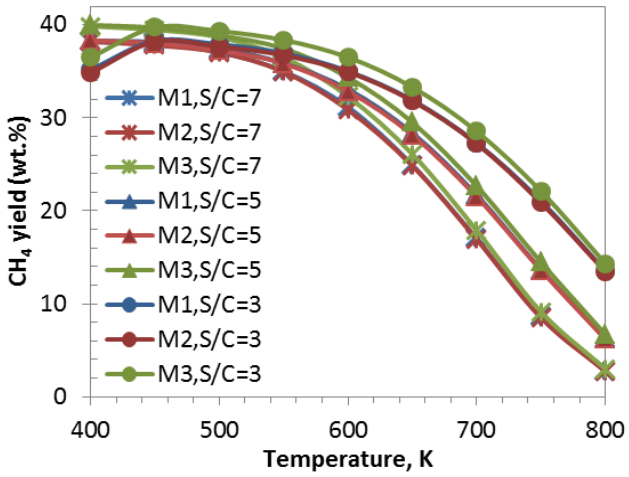

Figure 2. CH_4 yield (wt %) for three different PEFB bio-oil mixture compositions listed in Table 4 for S/C from 3 to 7 and 1 atm.

Subsequently, mixture M3, which contains only acetic acid and phenol, was chosen in this investigation to represent the LTSR and SE-LTSR of PEFB bio-oil since it gave the smallest percentage error in the theoretical maximum CH4 yield (1.13%) compared to the target bio-oil.

3.2. Thermodynamic equilibrium analysis of direct CH_4 production from PEFB bio-oil by LTSR with and without in situ CO_2 sorption

3.2.1. Expected outputs from stoichiometry of LTSR and SE-LTSR reactions and relevance to LTSR process design

The mixture M3 (Table 4) with the elemental formula $C_{0.3368}H_{0.4842}O_{0.1789}$ was chosen as the model mixture for PEFB bio-oil, and the generic global reaction of CH_4 production from bio-oil (in vapour state) with CO_2 as a co-product (R7), can be expressed by reaction (R13) using M3 as the feedstock:

$$C_{0.3368}H_{0.4842}O_{0.1789(G)}+0.126\ H_2O_{(G)}\rightarrow 0.153\ CO_2+0.184\ CH_4 \quad \Delta H_{298\ K} = -45.4\ kJ/mol\ CH_4 \qquad (R13)$$

Thus, LTSR of M3 as expressed by (R13) is significantly exothermic and therefore, there may be a potential for heat recovery to bring the reactants to reformer temperature and achieve a near-autothermal process. The stoichiometric molar steam to carbon ratio (S/C) was at a low value of 0.375 (= 0.1263/0.3368), corresponding to a maximum CH_4 yield of 40.0 wt % of M3, and associated with an ideal CH_4 purity of 54.7 mol % in the CH_4-CO_2 reformate mixture. By comparison, the S/C required for H_2 and CO_2 production through high-temperature steam reforming (HTSR) of M3 (S/C = 1.47) was significantly higher and would produce a maximum of H_2 yield of 20.1 wt % of M3.

When using $CaO_{(S)}$ as the CO_2 sorbent and combining the results of (R13) and (R9) in (R14), the SE-LTSR of M3 model PEFB bio-oil is:

$$C_{0.3368}H_{0.4842}O_{0.1789(G)} + 0.126\ H_2O_{(G)} + 0.153CaO_{(S)} \rightarrow 0.153CaCO_{3(S)} + 0.184\ CH_4$$
$$\Delta H_{298\ K} = -193.0\ kJ/mol\ CH_4 \qquad (R14)$$

Furthermore, when using $Ca(OH)_{2(S)}$ as the in situ CO_2 sorbent and combining the results of (R13) and (R10) in (R15), this potentially generates pure CH_4 reformate:

$$C_{0.3368}H_{0.4842}O_{0.1789(G)} - 0.026\ H_2O_{(G)} + 0.153Ca(OH)_{2(S)} \rightarrow 0.153CaCO_{3(S)} + 0.184\ CH_4$$
$$\Delta H_{298\ K} = -102.6\ kJ/mol\ CH_4 \qquad (R15)$$

High-temperature steam reforming (HTSR) for H_2 and CO_2 generation also has a stoichiometric Ca:C of 1 when coupled with in situ Ca-based CO_2 sorption. Thus, temperature and S/C variations in a reformer are expected to change rapidly from conditions favourable to SE-LTSR to those advantages for sorption enhanced-HTSR or 'SE-HTSR', where H_2 product is preferred over CH_4. In addition to improving reformate purity in H_2, in situ CO_2 capture has other benefits that have been identified in SE-HTSR: lower S/C for threshold of carbon formation, higher H_2 yields from equilibrium shifts in steam reforming and water gas shift reactions, lower overall energy demand from operating at lower S/C and T, a wider range of temperatures of maximum yield, collectively known as enhancement effects of sorption-enhanced steam reforming process (SESR) [18,35]. The present study aims to assess for the first time whether similar benefits can be observed for SE-LTSR in equilibrium production of pure methane reformate.

Unlike SE-HTSR, which always requires H_2O co-reactant whether $CaO_{(S)}$ or $Ca(OH)_{2(S)}$ is used as the sorbent, SE-LTSR theoretically does not need H_2O feed when using $Ca(OH)_{2(S)}$ because its

stoichiometric S/C for reaction R15 is negative (i.e. −0.026). The stoichiometric S/C of R14 and R15 differ greatly due to the sorbent in R15 being already hydrated, which is represented in the considerably exothermic reaction R16.

Hydration of $CaO_{(S)}$:

$$CaO_{(S)} + H_2O_{(G)} \leftrightarrows Ca(OH)_{2(S)} \qquad \Delta H_{298\,K} = -109.2\ \text{kJ/mol}\ CaO_{(S)} \qquad \text{(R16)}$$

When operating at temperatures approximately below 400 ℃, $CaO_{(S)}$ readily hydrates to $Ca(OH)_{2(S)}$, whereas above this temperature, $Ca(OH)_{2(S)}$ dehydration is favoured. Calcination of Ca-based CO_2 sorbents at around 900 ℃ via the reverse of (R9) enables the release of captured CO_2 from $CaCO_{3(S)}$, thereby regenerating the Ca-based sorbent for another carbonation cycle. Without such regeneration step, the sorbent would eventually reach full capacity for CO_2 intake and cease to be active for sorption-enhanced H_2 or CH_4 production.

Ca-based sorbents are, however, well known to deactivate significantly, principally via sintering through repeated cycles of calcination [36]. Many studies of sorption-enhanced reforming have investigated hydration of Ca-based sorbents as a means to counteract the deactivation caused by calcination-induced sintering. It has been found that direct hydration, i.e. direct use of hydrated Ca-sorbent for high-temperature CO_2 sorption is more effective than indirect hydration, whereby calcination in an inert atmosphere is employed between hydration and subsequent carbonation [37].

Such investigations are, however, dedicated to higher temperature processes than LTSR, such as syngas production or post-combustion CO_2 capture. Particular concerns for SE-LTSR will be the sensitivity of CH_4 yield to fluctuations in the operating S/C and to temperature, exacerbated by the exothermicity of R14 and R15. In adiabatic process conditions, the use of $CaO_{(S)}$ with LTSR will see the hydration reaction R16 takes place first, which will lower H_2O partial pressures, followed by R15. The heat release of R16 and R15 would raise the system temperature in two stages, potentially creating inhomogeneity in local S/C, with risks of carbon deposition where S/C would dip too low, or hydrogen production to the detriment of methane via SE-HTSR where S/C would rise too high.

In contrast, the adiabatic SE-LTSR process using $Ca(OH)_{2(S)}$ would provide a one-step temperature rise with a steady supply of excess steam as an intermediate product, as R15 exhibits a negative stoichiometric S/C, in addition to the fact that no exothermic $CaO_{(S)}$ hydration will take place in the reformer. Thus, $Ca(OH)_{2(S)}$ offers advantages over $CaO_{(S)}$ as the preferred sorbent to enter the adiabatic low-temperature steam reformer: controlled reactivation after calcination of the sorbent and a one-step exothermic process in the reformer. Nevertheless, whether $CaO_{(S)}$ or $Ca(OH)_{2(S)}$ is used, with both R14 and R15 being significantly exothermic, there is a risk that the adiabatic reformer temperature may reach the unwanted sorbent calcination mode through exotherms, thus switching off the in situ CO_2 capture. In comparison, in the isothermal (controlled cooled) LTSR process using $Ca(OH)_{2(S)}$, the heat released during SE-LTSR would ensure operating at set temperatures is favourable for carbonation, but maintaining a constant temperature inside the reformer housing hot solid carbonate would add complexity to process control and design.

As mentioned in Section 2.3, CH_4 production was predicted using two different types of problems in the CEA code, which were the ‘Assigned Temperature and Pressure’ (tp), i.e. the isothermal reactor, and the ‘Assigned Enthalpy and Pressure’ (hp), i.e. the adiabatic reactor. The results for ‘tp’ are presented first, and the ‘hp’ results are compared and discussed at the end of this section, as they are both relevant to practical issues as discussed above.

Table 5 lists the molar inputs corresponding to the bio-oil mixture model used in equilibrium calculations. Other reactants in the system feed (e.g. H_2O, Ca sorbents, negligible Ar) are then

defined by the molar ratios of Ca:C and H_2O:C used, and the latter is also termed S/C for steam to carbon ratio when no sorbent is used, as previously.

The theoretical maximum CH_4 production for the M3 model bio-oil mixture molar inputs of Table 5 would therefore be 1641 moles, and this would be accompanied by 1359 moles of CO_2 via R13, or 1359 moles of $CaCO_{3(S)}$ via R14 or R15, which would then require calcination of the Ca-sorbent, releasing the same moles in the form of CO_2.

Table 5. Molar inputs of reactants in mixture M3 based on 3000 of total moles of carbon input.

Compound	Input moles	C (moles)	H (moles)	O (moles)
Acetic acid (CH_3COOH)	656.25	1312.5	2625	1312.5
Phenol (C_6H_5OH)	281.25	1687.5	1687.5	281.25
Total	937.5	3000	4312.5	1593.75

3.2.2. Temperature and S/C effects on the equilibria of isothermal LTSR and SE-LTSR of PEFB bio-oil model

In this section, the effects of changing temperature between 400 and 800 K and S/C from 0.5 to 7.0 at atmospheric pressure were investigated on the equilibrium system in order to determine the optimum conditions for PEFB bio-oil conversion to CH_4 via LTSR. Isothermal process (as opposed to adiabatic process) is considered. The conditions of optimum CH_4 yield for LTSR were then compared to the process outputs, which introduced $Ca(OH)_{2(S)}$ as the CO_2 sorbent in the feed mixture, simulating isothermal SE-LTSR.

Figure 3(a) shows that values close to the theoretical maximum of 1641 moles of CH_4 can be produced by LTSR without sorbent for S/C $\geq$ 2 and temperatures $\leq$ 550 K. This threshold minimum S/C is itself much higher than the stoichiometric S/C of 0.375 from the intended reaction R13. The reason for this discrepancy in S/C for maximum CH_4 yield can be found in Figure 4(a), which shows carbon graphite as the main equilibrium carbon-containing product at low temperatures and S/C below 2. For temperatures below 650 K and all S/C, negligible CO was produced, as seen in Figure 4(b), with the only other carbon-containing co-products of methane being carbon graphite and CO_2 (Figure 4(c)). At temperatures above 650 K, H_2 becomes the dominant hydrogen-containing product, as seen in Figure 4(d), and it increased with S/C as per HTSR process, accompanied by CO and CO_2. The dominance of solid carbon at low temperatures, low S/C and hydrogen at higher temperatures results in a dome-shaped profile of methane yield with temperature (Figure 3(a)), whose top flattened and shifted towards lower temperatures as S/C increased. In order to avoid too high sensitivity of methane yield to fluctuations in either temperature or S/C in a practical isothermal LTSR process of PEFB bio-oil, given that it will be overall exothermic in the reformer and thus highly dependent on good cooling controls, it is thus recommended to operate the isothermal LTSR of PEFB bio-oil in the S/C range of 2.5 to 3, and between 450 and 550 K, where CH_4 yield plateaus.

In the presence of $Ca(OH)_{2(S)}$, the maximum CH_4 production reached the theoretical maximum at Ca:C = 0.5, i.e. close to the stoichiometric Ca:C of 0.45 as determined from the intended reaction R15 (Figure 3(b)). This condition used comparatively much less steam than the sorbent-free system

to achieve close to the theoretical maximum yield of CH_4. The SE-LTSR equilibrium process thus behaves very closely to the intended reaction R15. As in LTSR, CH_4 yield in the isothermal SE-LTSR process decreased at high temperatures due to the rise in hydrogen co-product (Figure 4(d)). In sharp contrast with LTSR, SE-LTSR has no solid carbon predicted at equilibrium. This is true except for the conditions of sub-stoichiometric Ca:C (< 0.453), which results in a lack of steam generation via R10 (see Figure 4(a)) and thus prevents carbon oxidation. SE-LTSR also features a lack of both CO and CO_2 as long as the Ca:C is at or above stoichiometry of R15 (Figures 4(c,d)). Thus, prevention of equilibrium solid carbon is a sorption-enhancement effect that SE-LTSR shares with SE-HTSR. The only impediment to reach the theoretical maximum of CH_4 production is that even at low temperatures (400–500 K), concurrent H_2 production occurs, though in a limited way. Surprisingly, this results in a medium temperature region where CH_4 production via LTSR exceeds slightly that of SE-LTSR in isothermal conditions.

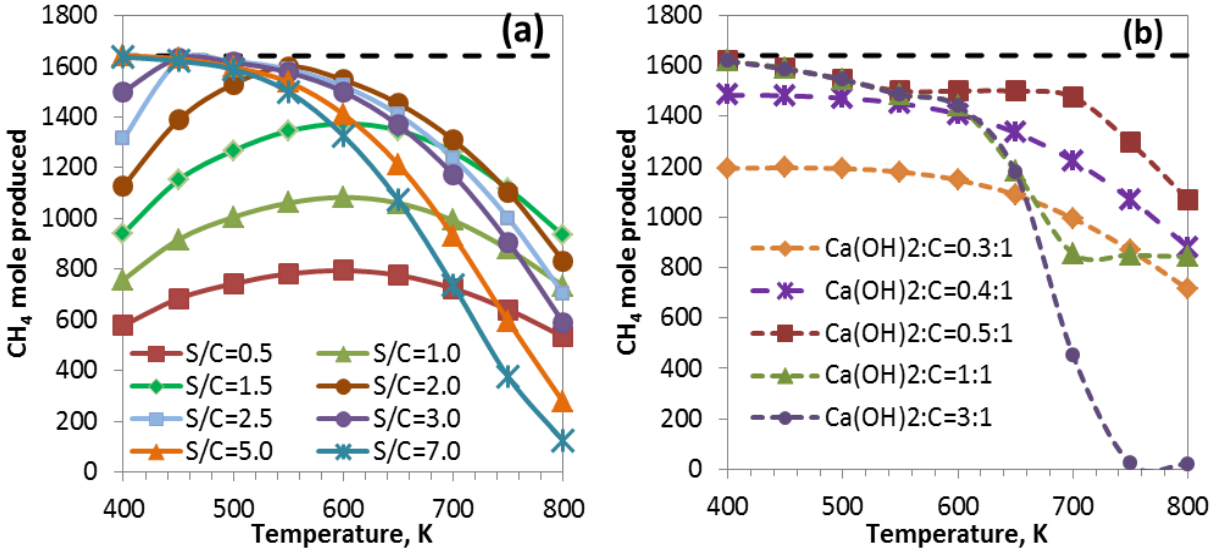

Figure 3. CH_4 production vs. temperature from M3 mixture (Table 5) without (a) and with $Ca(OH)_{2(S)}$ (b) at 1 atm. The top horizontal line is the theoretical maximum production via (R13).

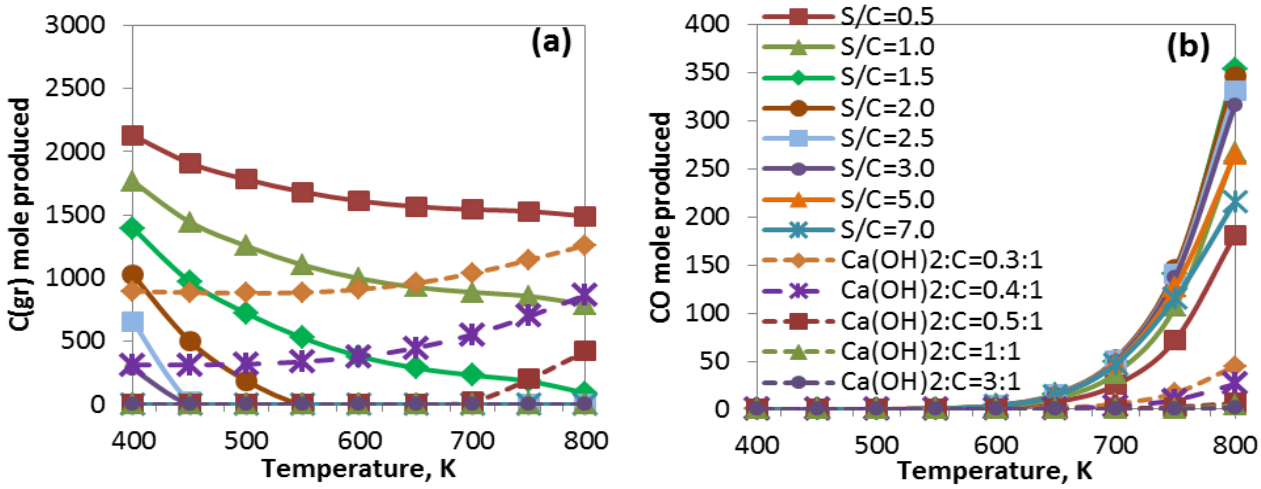

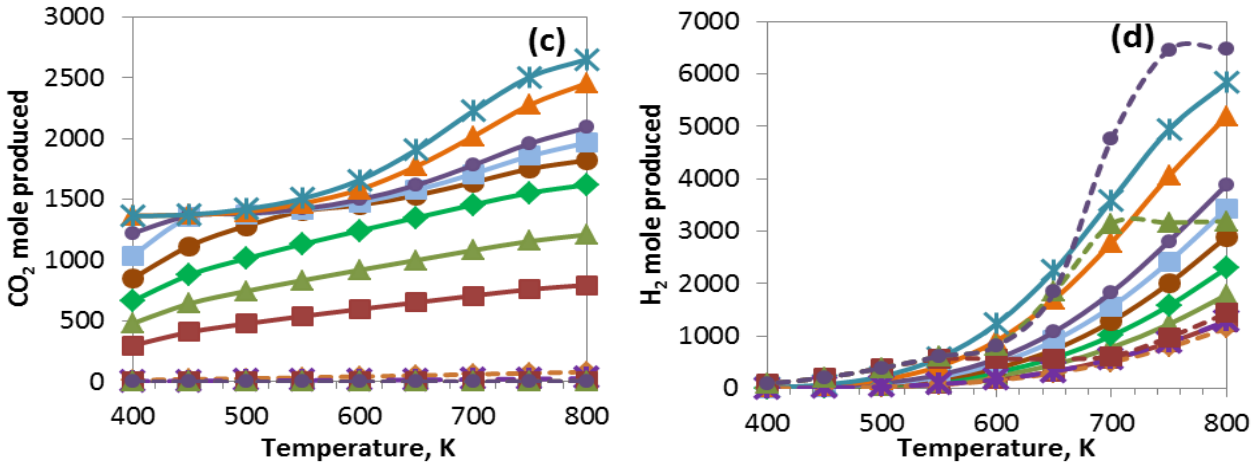

Figure 4. Production of (a) carbon graphite, (b) CO, (c) CO_2 and (d) H_2 between 400 and 800 K at 1 atm for LTSR (solid lines) and SE-LTSR (dashed lines) processes.

In theory, the use of a much lower S/C of SE-LTSR may result in energy cost savings by avoiding having to raise excess steam compared to LSTR. This issue will be explored in a later section (3.2.4). An immediate benefit of operating in SE-LTSR, however, is that the CH_4 in the dry reformate increased from 45 vol % with LTSR (S/C = 3) to 88 vol % with SE-LTSR (Ca:C = 0.5), when both at 450 K, i.e. at maximum CH_4 yield. This high level of purity in the reformer may or may not remove the need for a CH_4 separation step downstream of SE-LTSR process, depending on the intended use for the CH_4 produced. However, the absence of a downstream CH_4 separation step may itself be mitigated by having to introduce a sorbent regeneration measure, also downstream of the reformer. Incidentally, the sorption enhancement effect on HTSR can be seen in the high temperature range (> 650 K) by the decrease in CO and increase in H_2 production due to the more favourable equilibrium in the water gas shift reaction (R3) caused by the removal of CO_2 from the products via carbonation. The latter was observed experimentally, as well as equilibrium modelling in [18].

As discussed earlier in Section 3.2.1, there are a number of advantages in potentially rating $Ca(OH)_{2(S)}$ above $CaO_{(S)}$ as the active sorbent in the isothermal SE-LTSR process. These are relevant to the stability of both temperature and S/C in the cooled reformer by eliminating $CaO_{(S)}$ hydration through reaction R16. Inhomogeneity in temperature and S/C caused by the heat released by R16 and water demand may result in either local carbon formation or too high H_2 co-product. When replacing $Ca(OH)_{2(S)}$ with $CaO_{(S)}$ in the system and adding the required equivalent H_2O co-reactant separately, the same production profiles of CH_4, CO, C and H_2 for $Ca(OH)_{2(S)}$ based SE-LTSR were obtained, and thus the results for $CaO_{(S)}$ based SE-LTSR are not shown here. This is because in isothermal conditions below 700 K, i.e. LTSR conditions, the hydration reaction R16 is complete in excess of steam conditions.

3.2.3. Pressure effects in the equilibria of isothermal LTSR and SE-LTSR of PEFB bio-oil model

Methane synthesis exothermic reactions (R4-R6) involve the production of less moles of gas products than the initial moles of reactant. According to Le Chatelier's principle, an increase in pressure will imbalance the reactants more than the products and the system equilibrium will counteract this change by increasing conversion. This effect can be seen in Figure 5, where

increasing the system pressure from 1 to 30 atm at S/C of 3 brings the profile of CH_4 product closer to the theoretical maximum. An industrial process of LTSR of PEFB would therefore benefit in terms of CH_4 yield from operating at higher pressures than atmospheric, with pressure of just 5 atm significantly expanding the temperature zone of maximum CH_4 yield compared to 1 atm by approximately 60 K, and compared to 30 atm by 150 K from its starting point of optimum temperature. This could be advantageous in the industrial process where the kinetics of methanation catalyst may be very sensitive to temperature in the range of maximum equilibrium CH_4 yield, and activity at 550 K could be significantly lower than at 610 K (5 atm) or 700 K (30 atm). The drawback of operating at higher pressures would be in the increased boiling point of the reactants, the resulting surge in energy demand for vaporisation of liquid water feed.

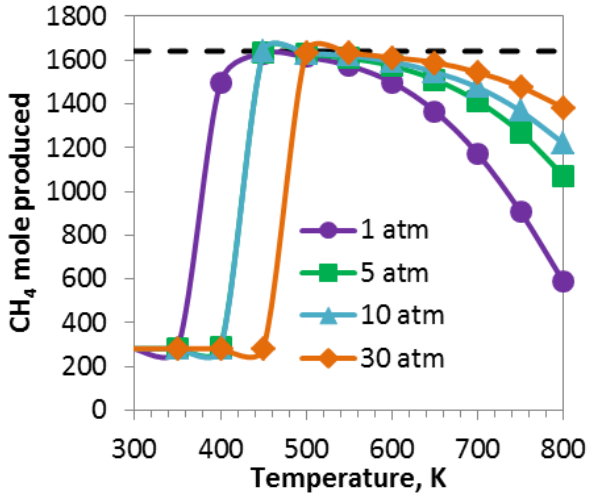

Figure 5. CH_4 production within 300–800 K at S/C = 3.0 for total pressures between 1 and 30 atm. The top horizontal line is the theoretical maximum production via (R13).

3.2.4. Enthalpy balances for the equilibria of isothermal LTSR and SE-LTSR of PEFB bio-oil model

The main global reactions that are related to the LTSR process for CH_4 production from the M3 model bio-oil mixture, such as several CH_4 synthesis reactions (R4–R6, R13–R15), water-gas shift, hydration of CaO, and carbonation of both CaO and $Ca(OH)_2$, are listed in Table 6 with their standard enthalpies of reaction. The overall process for isothermal CH_4 production via LTSR is expected to be exothermic in the reformer since all of the reactions involved exhibit negative value of reaction enthalpy. In the process start-up, using reactants at ambient temperature and natural phases will introduce a significant heat demand to first, vaporise volatile reactants in condensed phases (net liquid water, liquid acetic acid and crystalline phenol) and secondly, bringing all the reactants in the vapour phase to reformer temperature. Beyond start-up conditions, however, the process will operate cyclically, where solids will be regenerated from carbonate state to oxide and excess water will be used either to rehydrate CaO or used as a reforming co-reactant. In order to represent ideal processes where heat recuperation has 100% efficiency, we will assume that

decarbonation occurs at reformer temperature (in practice, temperature in excess of 900 ℃ is typically required), and thus solids and water recycling will not incur sensible enthalpy changes, but only reaction enthalpy changes. This section looks at the total heat demand of LTSR compared to SE-LTSR.

Table 6. Reaction of enthalpy (ΔH_R) for main global reactions that are related to LTSR for methane production at 298 K (M3 = $C_{0.3368}H_{0.482}O_{0.1789(G)}$).

	Reaction	Stoichiometry (mol)	$\Delta H_{298\ K}$ (kJ)
R3	Water gas-shift	$CO + H_2O_{(G)} \leftrightarrows CO_2 + H_2$	−41.2/mol CO
R4	Methanation of CO	$CO + 3H_2 \leftrightarrows CH_4 + H_2O_{(G)}$	−206.2/mol CH_4
R5	As above	$2CO + 2H_2 \leftrightarrows CH_4 + CO_2$	−247.3/mol CH_4
R6	Methanation of CO_2	$CO_2 + 4H_2 \leftrightarrows CH_4 + 2H_2O_{(G)}$	−165.0/mol CH_4
R9	Carbonation of CaO	$CaO_{(S)} + CO_2 \leftrightarrows CaCO_{3(S)}$	−178.2/mol CO_2
R12	Carbonation of $Ca(OH)_2$	$Ca(OH)_{2(S)} + CO_2 \leftrightarrows CaCO_{3(S)} + H_2O$	−69.0/mol CO_2
R13	LTSR of M3 bio-oil	$M3 + 0.126\ H_2O \rightarrow 0.153CO_2 + 0.184\ CH_4$	−45.4/mol CH_4
R14	SE-LTSR, $CaO_{(S)}$	$M3 + 0.126H_2O + 0.153CaO_{(S)} \rightarrow 0.153CaCO_{3(S)} + 0.184CH_4$	−193.0/mol CH_4
R15	SE-LTSR, $Ca(OH)_{2(S)}$	$M3 - 0.026H_2O + 0.153Ca(OH)_{2(S)} \rightarrow$ as (R14)	−102.6/mol CH_4
R16	Hydration of CaO	$CaO_{(S)} + H_2O_{(G)} \leftrightarrows Ca(OH)_2$	−109.2/mol H_2O

Figure 6 plots ΔH_{Tot} derived from equation (11) for the isothermal LTSR and SE-LTSR cases at atmospheric pressure. We remind that ΔH_{Tot} is the sum of enthalpy changes of raising bio-oil and net water reactants from their natural phases from 298 K to vapour state at reforming temperature T and the reaction enthalpy change at T, as well as calcination enthalpy change at T, if carbonate was present in the products, with rehydration of $CaO_{(S)}$ product in the case of the calcium hydroxide sorbent used as the reactant, and dehydration in the case of $Ca(OH)_{2(S)}$ product and calcium oxide used as the reactant. From previous thermodynamic equilibrium calculations, SE-LTSR with Ca:C = 0.5:1 and LTSR with S/C = 3.0 were identified as the optimum conditions for maximum CH_4 production, with their maxima reached within the temperature interval of 400–600 K. In this section, the two processes are further compared in terms of individual energy terms for reforming temperature at 450 K (see Table 7) in order to determine the conditions that could potentially provide more energy savings for CH_4 production.

From Figure 6, for LTSR and SE-LTSR, the total ΔH for producing one mole of CH_4 increased with temperature. This was caused by an increase in the reactants ΔH calculated using equation (6), as well as an increase in ΔH of reaction, which evolved from very exothermic due to carbon graphite co-product to very endothermic due to H_2 co-product. In the maximum methane production region for LTSR (S/C = 3, T = 450 K), ΔH_{Tot} was 31.3 kJ/mol CH_4, resulting from 75.2 kJ/mol CH_4 produced which attributed to reactants heating demand, and −44 kJ/mol CH_4 of exothermic reaction in the reformer (Table 5). By comparison, at the maximum methane production for SE-LTSR ($Ca(OH)_2$:C = 0.5:1, 450 K), the total ΔH_{Tot} of 37.2 kJ/mol of CH_4 produced was the result of a very exothermic reaction ΔH of −104 kJ/mol CH_4, overwhelmed later by a strongly endothermic decarbonation of the sorbent (+157.1 kJ/mol CH_4), with the other terms (reactants heating $\Delta H > 0$, rehydration of $CaO_{(S)} < 0$) roughly cancelling each other.

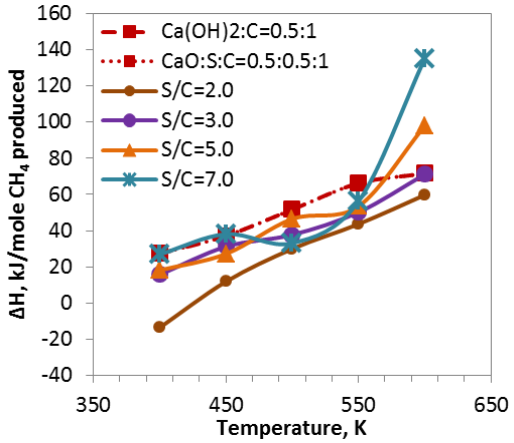

Figure 6. Total enthalpy (ΔH_{Tot}) for producing 1 mole of CH_4 from bio-oil steam reforming for LTSR in the range of S/C = 2–7, SE-LTSR using $Ca(OH)_2$:C = 0.5:1 (no inlet steam) and CaO:S:C = 0.5:0.5:1 for reformer temperatures of 400–600 K at 1 atm. (S = steam)

The results shown in Figure 6 and Table 7 assume ideal heat recuperation conditions when recycling water and regenerated sorbent to the reformer and therefore, there are no great differences in ΔH_{Tot} for a given reforming temperature when S/C varies from 2 to 7. In practice, the ΔH_{Tot} of LTSR would significantly increase with S/C had more realistic recycling and heat recuperation conditions been considered. This is now illustrated in the worst case scenario of LTSR without recycling or heat recuperation of water, for which the calculated ΔH_{Tot} at S/C of 2 was 202 kJ per mol CH_4 produced, rising to 268 and 639 kJ/mol CH_4 at S/C of 3 and 7, respectively, for similar reforming temperature of 450 K (results are not shown in figure or table). Similarly, SE-LTSR's heat demand would also increase significantly as decarbonation above 1170 K (calcination by oxy-combustion, for example) followed by non-ideal cooling of $CaO_{(S)}$, and subsequently by its rehydration and recycling that would introduce heat and material losses. Again, in the worst case scenario of SE-LTSR where decarbonation is conducted at 1170 K, and neither the sorbent nor the water or their heat is recycled, the ΔH_{Tot} of SE-LTSR with $CaO_{(S)}$ as the sorbent would be 381 kJ per mol CH_4 produced.

Table 7 lists the ΔH_{Tot} of LTSR and SE-LTSR at atmospheric pressure, but similar calculations were performed at 30 atm (not shown). It was found that the ΔH_{Tot} of isothermal LTSR and SE-LTSR in ideal conditions of recycle and heat recuperation was approximately 28–29 kJ per mol of CH_4 produced, with the differences of 1 atm found mainly in the 'reaction ΔH' term for LTSR and 'decarbonation ΔH' for SE-LTSR, indicating modest pressure effect on the enthalpy balance. More significant benefits of lower energy costs were observed when operating at higher temperatures (up to 600 K) when comparing 30 atm with 1 atm conditions due to the higher maximum CH_4 yield at 30 atm (as seen in Figure 5).

Given the difficulties in recycling solid sorbent streams that becomes worse at high pressure (blockages at valves, risks of compromised seals) and for efficiently recuperating their heat, and also due to the fact that the reformate product of SE-LTSR may still require further purification post-processing stage to remove H_2 impurities and uncaptured CO_2, there seem to be no clear advantages of SE-LTSR over LTSR in isothermal conditions, where both are expected to produce maximum CH_4 amounts.

Table 7. Enthalpy change terms for 1 mole of CH_4 produced by isothermal LTSR at S/C of 3 and isothermal SE-LTSR with Ca:C of 0.5:1 (with CaO and $Ca(OH)_2$ as sorbents) at 1 atm. All calculations were done at 450 K and ΔH terms were given in kJ/mol of CH_4.

Equation	Enthalpy change term	Initial state → Final state	LTSR S/C = 3	CaO-LTSR 0.5:0.5:1	$Ca(OH)_{2(S)}$-LTSR 0.5:1
Eq. 4	Acetic acid ΔH	298 K (l) → (g) 450 K	25.3	25.9	25.9
Eq. 4	Phenol ΔH	298 K (s) → (g) 450 K	15.2	15.6	15.6
Eq. 5	H_2O ΔH	298 K (l) → (g) 450 K	34.7	38.0	N/A
Eq. 7	Reaction ΔH	450 K (g) → (g) 450 K	−43.9	−205.4	−104.4
Eq. 8	Decarb ΔH	450 K (s) → (s) 450 K	0.0	157.1	157.1
Eq.9	DeHy ΔH	450 K (s) → (s) 450 K	N/A	6.0	N/A
Eq. 10.1	ReHy1 ΔH	450 K (l,s) → 450 K (s)	N/A	N/A	−12.3
Eq. 10.2	ReHy2 ΔH	(s) 450 K&(l)298 K→(s) 450 K	N/A	N/A	−44.6
Eq. 11	ΔH_{Tot}	298K (l,s) → (g,s) 450 K	31.3	37.2	37.2

The recommendation thus remains that for the isothermal process, LTSR at S/C of 3 (in order to clearly avoid equilibrium solid carbon product) and temperatures between 450 and 500 K, be utilised in combination with each other, as they provide more energy efficient and high methane yield conditions. Operating at higher pressures than atmospheric would bring about higher yields but also higher costs associated with fluid movers and reactor vessel specifications. These conditions will then require moderate heating in order to maintain the desired temperature.

3.2.5. Comparison between isothermal and adiabatic LTSR processes for CH_4 production from PEFB bio-oil model

As mentioned earlier, the 'hp' problem (i.e. constant enthalpy, constant pressure) was also conducted in the CEA programme to simulate the adiabatic LTSR and SE-LTSR processes (i.e. without heat losses, representing a well-insulated reformer without internal cooling). Figure 7 shows CH_4 production at varying S/C and temperatures for the adiabatic LTSR process at 1 atm. CH_4 production was favoured at lower initial temperatures (400–550 K) than the isothermal process, and the optimum conditions for CH_4 production were obtained at and above S/C = 2. This was caused by the significant increase in the equilibrium temperature of the adiabatic process (Figure 8) at low initial temperatures compared to the isothermal process, thus avoiding carbon graphite and CO by-products for S/C above 2 (C and CO not shown). If operating LTSR in adiabatic conditions from low initial temperature is possible in practice, higher yield of CH_4 than in the isothermal case would be obtained, as the dome-shaped methane production with temperature shifted to the left due to the heat released in the reformer hampering the carbon graphite by-product as long as there is sufficient steam co-reactant. In reality, as inlet temperatures fall towards ambient conditions (where the theoretical benefits on adiabatic equilibrium CH_4 yield have been found compared to the isothermal case), the bio-oil mixture will risk entering the reformer in liquid form, thus most likely deactivating the catalyst. In addition, kinetic rates of the catalytic reactions at low input temperatures will fall drastically and the exotherms on which the process relies may not occur. Thus, operating the adiabatic reactor would still require significant input temperatures in the reformer to guarantee

adequate vapour phase of bio-oil components and significant catalytic activity.

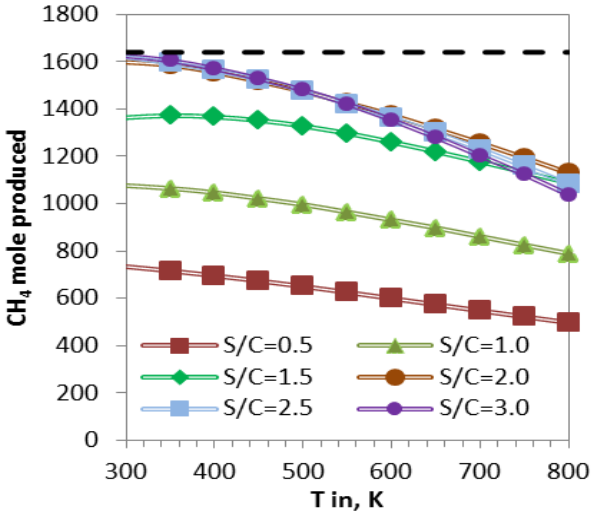

Figure 7. CH_4 production for adiabatic LTSR within 300–800 K at 1 atm. This figure is to be compared to Figure 2(a) of the isothermal case.

To conclude our comparison between isothermal and adiabatic LTSR processes without CO_2 sorbent, the reality will most likely reflect a hybrid case; not fully adiabatic, hence, close to isothermal. Therefore, the recommended operating conditions of LTSR in order to ensure reactants in vapour phase are in contact with the active catalyst in the reformer are an adiabatic reactor with downstream heat and water recuperation from the reformate of S/C of 3 and inlet temperature of ca. 450 K (177 ℃) whether at 1 atm or higher. This will help to meet the overall moderate energy costs dominated by heating up the reactants whilst the reformer temperature may rise to 582 K (309 ℃) as a result of exothermic reforming.

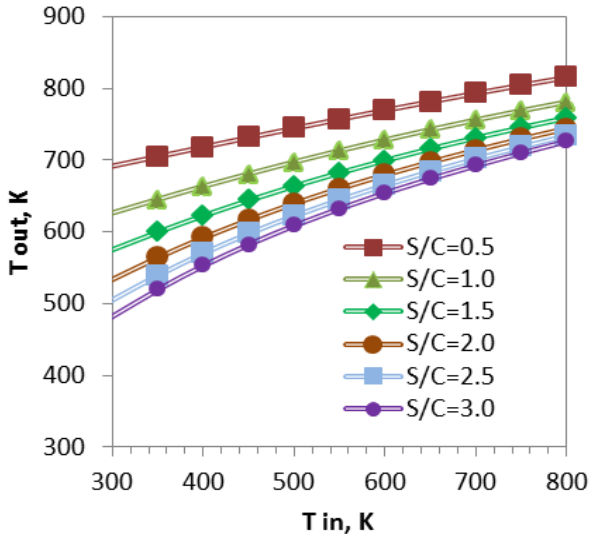

Figure 8. Temperature output of the process for different values of S/C ratio (1–3) within 300–800 K of input temperature at 1 atm.

Based on Figure 9, CH_4 production with $CaO_{(S)}$ in the SE-LTSR process in adiabatic and isobaric conditions (hp) was far below both the theoretical maximum and equilibrium CH_4 produced in the isothermal-isobaric (tp) case. This is due to the predicted equilibrium temperatures being much higher than the initial temperatures (above 900 K, Figure 9(b)), which, despite being favourable for CO_2-capture by very exothermic carbonation, as evidenced by the significant carbonate product profiles in Figure 9(b), moved the process in SE-HTSR regime, benefitting H_2 to the detriment of CH_4 production.

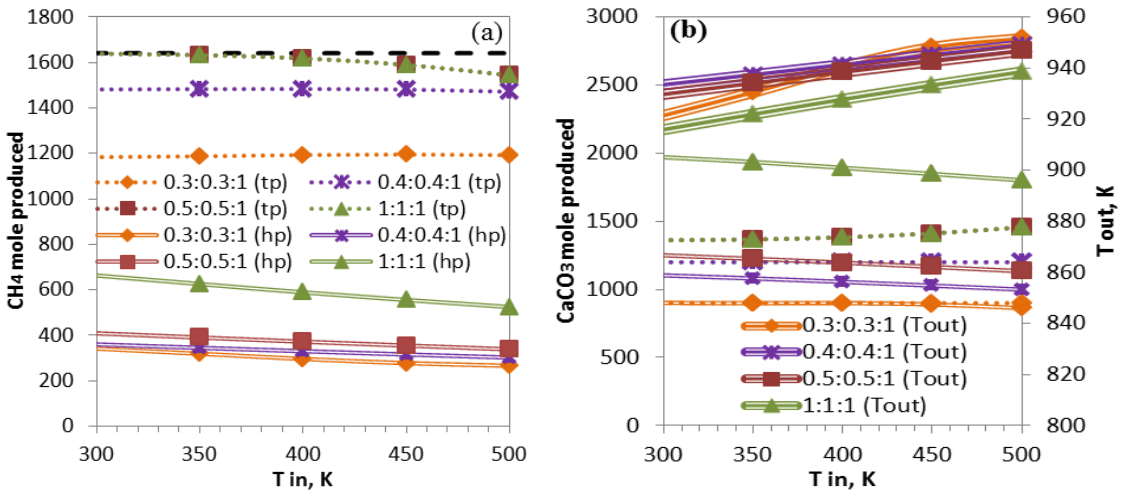

Figure 9. CH_4 production (a) and $CaCO_3$ production and equilibrium temperature (b) in the isothermal (tp) and adiabatic (hp) cases for SE-LTSR using CaO as CO_2 sorbent within 300–800 K at 1 atm. The top line in (a) is the theoretical maximum. The format of molar ratio is presented in CaO:H_2O:C. (S = steam)

Consequently, adiabatic SE-LTSR would not be achievable in practice, as the large temperature increase caused by carbonation would only allow for SE-HTSR, with minimal methane production. Given the large heat released for both $CaO_{(S)}$ and $Ca(OH)_{2(S)}$ SE-LTSR per mole of CH_4 produced, in practice, isothermal SE-LTSR would introduce major reactor design complexities from having to internally cool down the reformer, in which solid sorbents are the main source of heat due to carbonation. The only advantage of isothermal SE-LTSR over adiabatic LTSR would be the production of reformate with high methane concentration from the reactor, although small amounts of H_2 would still be present. This benefit is here considered insufficient to countermand the challenges posed by process solid flow recycling and heat recuperation. The final recommendation is therefore to operate at close to adiabatic LTSR with S/C of 3 and inlet temperature of ca. 450 K to achieve CH_4 yield of 38.3 wt %, i.e. near the theoretical maximum of 40 wt %, with a reformate dry composition of 44.5 vol % CH_4, 42.7 vol % CO_2 and 12.7 vol % H_2. This process would then lend itself to post-process CO_2 capture via CH_4 purification, and this may influence the choice of pressure for the reformer. The moderate heat demand of the LTSR process in bringing the reactants to vapour phase may be partly met if an on-site pyrolysis/LTSR process is designed, where the volatiles from the PEFB pyrolysis stage are directed with little heat loss to a nearby LTSR stage, and only the vapour co-reactant would require heating/vaporising with excess steam being recycled.

4. Conclusion

PEFB bio-oil has the potential to be converted into CH_4 via the low-temperature steam reforming (LTSR) process. CH_4 production was favoured in the 400–600 K range at atmospheric pressure with and without CO_2 sorption. The large exothermicity of SE-LTSR precluded this process to be recommended, as the adiabatic reactor produced more H_2 than CH_4. Furthermore, isothermal SE-LTSR would require costly internal cooling capability, as well as solids and heat recuperation design features for the small benefit of producing a reformate with high CH_4 concentration. Therefore, the optimum conditions of CH_4 production can be achieved by operating LTSR at around molar steam to carbon ratio of 3, with inlet temperature of ca. 450 K (or lower, if allowed by the catalyst activity and vapour state of the reactants), with efficient water recycle and heat recuperation from wet reformate. Pressures higher than atmospheric would contribute to reaching close to maximum CH_4 yields at higher temperatures. These conditions would have a moderate overall heat demand, whilst producing near the theoretical maximum CH_4, albeit with a purity of ca. 45 vol %.

Acknowledgements

The authors would like to thank the Education of Malaysia (EM) for the financial support for the PhD student Hafizah Abdul Halim Yun.

Conflict of interest

All authors declare no conflict of interest in this paper.

References

1. Balat M (2008) Mechanisms of thermochemical biomass conversion processes. Part 1: Reactions of pyrolysis. *Energ source part a* 30: 620–635.
2. Sulaiman F, Abdullah N (2011) Optimum conditions for maximizing pyrolysis liquids of oil palm empty fruit bunches. *Energy* 36: 2352–2359.
3. Mohan D, Pittman CU, Steele PH (2006) Pyrolysis of wood/biomass for bio-oil: A critical review. *Energ fuel* 20: 848–889.
4. Bridgewater AV (2012) Review of fast pyrolysis of biomass and product upgrading. *Biomass bioenerg* 38: 68–94.
5. Zhang R, Cummer K, Suby A, et al. (2005) Biomass-derived hydrogen from an air-blown gasifier. *Fuel process technol* 86: 861–874.
6. Sulaiman F, Abdullah N, Gerhauser H, et al. (2011) Review: An outlook of Malaysian energy, oil palm industry and its utilization of wastes as useful resources. *Biomass bioenerg* 35: 3775–3786.
7. Badger PC, Fransham P (2006) Use of mobile fast pyrolysis plants to densify biomass and reduce biomass handling costs-a preliminary assessment. *Biomass bioenerg* 20: 321–325.
8. Czernik S, Bridgewater AV (2004) Overview of applications of biomass fast pyrolysis oil. *Energ fuel* 18: 590–598.
9. Kopyscinski J, Schildhauer TJ, Biollaz SMA (2010) Production of synthetic natural gas (SNG) from coal and dry biomass: A technology review from 1950 to 2009. *Fuel* 89: 1763–1783.

10. National Renewable Energy Laboratory (US). Energy analysis biogas potential in the United States. Colorado (US): U.S. Department of Energy (US); 2013. 4 p. (NREL publication; no. NREL/FS-6A20-60178).
11. AEBIOM European Biomass Association. A biogas road map for Europe. Belgium: Renewable Energy House, Rue d'Arlon, Brussels; 2009 October. Available from: http://www.aebiom.org/IMG/pdf/Brochure_BiogasRoadmap_WEB.pdf.
12. Kelleher Environmental. Benefits to the economy, environment and energy. Canada: The Biogas Association; 2013 November. Available from: http://www.biogasassociation.ca/bioExp/images/uploads/documents/2013/resources/Canadian_Biogas_Study_Summary.pdf.
13. BP. BP Statistical Review of World Energy June 2015. UK: Heriot-Watt University; 2015 June. Available from: http://www.bp.com/content/dam/bp-country/de_de/PDFs/brochures/bp-statistical-review-of-world-energy-2015-full-report.pdf
14. Suruhanjaya Tenaga (Energy Commission). National Energy Balance 2013. Malaysia: Energy Commission, Putrajaya; 2014 March. Available from: http://meih.st.gov.my/documents/10620/167a0433-510c-4a4e-81cd-fb178dcb156f
15. Beer T, Grant T, Brown R. Life-cycle emissions analysis of alternative fuels for heavy vehicles. Australia: Australian Greenhouse Office; 2000. 148p. (CSIRO Atmospheric Research report; no. C/0411/1.1/F2).
16. Van der Meijden CM, Veringa H, Vreugdenhill BJ, et al. (2009) Production of bio-methane from woody biomass. Available from: http://www.ecn.nl/docs/library/report/2009/m09086.pdf.
17. Xie H, Yu Q, Wei M, et al. (2015) Hydrogen production from steam reforming of simulated bio-oil over Ce-Ni/Co catalyst with in continuous CO2 capture. *Int j hydrogen energ* 40: 1420–1428.
18. Md Zin R, Lea-Langton A, Dupont V, et al. (2012) High hydrogen yield and purity from palm empty fruit bunch and pine pyrolysis oils. *Int j hydrogen energ* 37: 10627–10638.
19. Remon J, Broust F, Volle G, et al. (2015) Hydrogen production from pine and poplar bio-oils by catalytic steam reforming. Influence of the bio-oil composition on the process. *Int j hydrogen energ* 40: 5593–5608.
20. Xie H, Yu Q, Wang K, et al. (2014) Thermodynamic analysis of hydrogen production from model compounds of bio-oil through steam reforming. *Environ prog sustain energy* 33: 1008–1016.
21. Department of Energy and Climate Change. Digest of United Kingdom Energy Statistics 2014. London: The National Archives; 2014. Available from: https://www.gov.uk/government/uploads/system/uploads/attachment_data/file/338750/DUKES_2014_printed.pdf
22. Oh TH, Pang SH, Chua SC (2010) Energy policy and alternative energy in Malaysia: Issues and challenges for sustainable growth. *Renew sust energ rev* 14: 1241–1252.
23. Hosseini SE, Abdul Wahid M (2013) Feasibility study of biogas production and utilization as a source of renewable energy in Malaysia. *Renew sust energ rev* 19: 454–462.
24. Subramaniam V, Ngan MA, May CY, et al. (2008) Environmental performance of the milling process of Malaysian palm oil using the life cycle assessment approach. *American j environ sci* 4: 310–315.

25. Prasertsan S, Prasertsan P (1996) Biomass residues from palm oil mills in Thailand: An overview on quantity and potential usage. *Biomass bioenerg* 11: 387–395.
26. Van der Meijden CM, Veringa HJ, Rabou LPLM (2010) The production of synthetic natural gas (SNG): A comparison of three wood gasification systems for energy balance and overall efficiency. *Biomass bioenerg* 32: 302–311
27. Ni M, Leung DYC, Leung MKH, et al. (2006) An overview of hydrogen production from biomass. *Fuel process technol* 87: 461–472.
28. Bridgewater AV (2012) Review of fast pyrolysis of biomass and product upgrading. *Biomass bioenerg* 38: 68–94.
29. Sukiran MA, Chin CM, Abu Bakar NK (2009) Bio-oils from pyrolysis of oil palm empty fruit bunches. *American j appl sci* 6: 869–875.
30. Abdullah N, Sulaiman F, Gerhauser H (2011) Characterisation of oil palm empty fruit bunches for fuel application. *J phys sci* 22: 1–24.
31. Abdullah N, Gerhauser H, Bridgwater AV (2007) Bio-oil from fast pyrolysis of oil palm empty fruit bunches. *J phys sci* 18: 57–74.
32. Gu H, Song G, Xiao J, et al. (2013) Thermodynamic analysis of the biomass-to-synthetic natural gas using chemical looping technology with CaO sorbent. *Energ fuel* 27: 4695–4704.
33. Zeleznik FJ, Gordon S. An analytical investigation of three general methods of calculating chemical-equilibrium compositions. Ohio (US): National Aeronautics and Space Administration (US); 1960. 37p. (NASA publication; no. NASA TN D-43).
34. Gordon S, McBride BJ. Computer program for calculation of complex chemical equilibrium compositions and applications: I. Analysis. Ohio (US): National Aeronautics and Space Administration (US); 1994. 58p. (NASA publication; no. NASA RP-1311).
35. Dupont V, Twigg MV, Rollinson AN, et al. (2013) Thermodynamics of hydrogen production from urea by steam reforming with and without in situ carbon dioxide sorption. *Int j hydrogen energ* 38: 10260–10269.
36. Wang Q, Luo J, Zhong Z, et al. (2011) CO_2 capture by solid adsorbents and their applications: current status and new trends. *Energ environ sci* 4: 42–55.
37. Blamey J, Manovic V, Anthony EJ, et al. (2015) On steam hydration of CaO-based sorbent cycled for CO_2 capture. *Fuel* 150: 269–277.

AIMS Press